ANALYTICAL SCIENCES APRIL 2016, VOL. 32

Consideration of Inner and Outer Phase Configuration in Tube Radial Distribution Phenomenon Based on Viscous Dissipation in a Microfluidic Flow Using Various Types of Mixed Solvent Solutions

Satoshi FUJINAGA,* Masahiko HASHIMOTO,* Kazuhiko TSUKAGOSHI,*,† and Jiro MIZUSHIMA*****

**Department of Chemical Engineering and Materials Science, Faculty of Science and Engineering, Doshisha University, Kyotanabe, Kyoto 610-0321, Japan*
***Tube Radial Distribution Phenomenon Research Center, Doshisha University, Kyotanabe, Kyoto 610-0321, Japan*
****Department of Mechanical and Systems Engineering, Faculty of Science and Engineering, Doshisha University, Kyotanabe, Kyoto 610-0321, Japan*

When mixed solvent solutions, such as ternary water–hydrophilic/hydrophobic organic solvents, water–surfactant, and water–ionic liquid, are delivered into a microspace under laminar flow conditions, the solvent molecules radially distribute in the microspace, generating inner and outer phases. This specific fluidic behavior is termed "tube radial distribution phenomenon", and has been used in separation technologies such as chromatography and extraction. The factors influencing the configuration of the inner and outer phases in "tube radial distribution phenomenon" using the above-mentioned mixed solvent solutions were considered from the viewpoint of viscous dissipation in fluidic flows. When the difference in the viscosity between the two phases was large (approximately >0.73 mPa·s), the phase with the higher viscosity formed as an inner phase regardless of the volume ratio. The distribution pattern of the solvents was supported by the viscous dissipation principle. Contrarily, when the difference was small (approximately <0.49 mPa·s), the phase with the larger volume formed as the inner phase. The distribution pattern of the solvents did not always correspond to the viscous dissipation principle. The current findings are expected to be useful in analytical science including microflow analysis research.

Keywords Phase separation multi-phase flow (PS-MPF), two-phase separation mixed solvent solution, tube radial distribution phenomenon (TRDP), tube radial distribution flow (TRDF), viscous dissipation

(Received September 25, 2015; Accepted December 14, 2015; Published April 10, 2016)

Introduction

Fluidic flows in a tube have been typically classified into two groups since the nineteenth century: homogeneous single-phase flows without a liquid–liquid interface[1,2] and immiscible multi-phase flows featuring a liquid–liquid interface.[3] Electroosmotic and laminar flows generated in a microspace, such as microchannels on a microchip and capillary tubes, are classified as homogeneous single-phase flows. In the last century, capillary electrophoresis[4] and hydrodynamic chromatography[5] were developed by taking advantage of electroosmotic flows and laminar flows, respectively. Recently, various types of immiscible multi-phase flows that can generate liquid–liquid interfaces have been reported with a relatively large inner diameter (several hundred μm) by using water and hydrophobic organic solvents.[6-9] The multi-phase flows show droplet, slug, parallel, or annular flows depending on the conditions employed.

We have recently developed a method to generate a multi-phase flow using two-phase separation mixed solvent solutions[10-14] such as ternary water–hydrophilic/hydrophobic organic solvent mixed solution, water–micelle mixed solution, water–ionic liquid mixed solution, and fluorocarbon/hydrocarbon organic solvent mixed solution. These new types of multi-phase flows are called "phase separation multi-phase flows" (PS-MPFs), and differ from the conventional "immiscible multi-phase flow". In PS-MPF, a homogeneous two-phase separation solvent solution is fed into a microspace, and then the solvent solution converts into a heterogeneous solution through phase transformation by changing the temperature and/or pressure, generating a liquid–liquid interface between the two phases.[10-14] We can also observe droplet, slug, parallel, or annular flow under different conditions in PS-MPF.

There is quite a difference in the interfacial tension between the conventional immiscible multi-phase flow and novel PS-MPF. The interfacial tension of PS-MPF (~0.7 – 3.3 mN m^{-1})[15] is considerably smaller than that of the immiscible multi-phase flow (~27 – 43 mN m^{-1}).[6-9] The small interfacial tension leads to a specific stable liquid–liquid interface even in a microspace and at low velocities.[13,16] Particularly, we are interested in the annular flow generated in PS-MPF. The solvent molecules are

† To whom correspondence should be addressed.
E-mail: ktsukago@mail.doshisha.ac.jp

radially distributed through the phase transformation of the two-phase mixed solvent solution, thus generating inner and outer phases to produce an annular flow. The specific microfluidic phenomenon and flow are termed "tube radial distribution phenomenon" (TRDP) and "tube radial distribution flow" (TRDF), respectively. The TRDP or TRDF has been applied to chromatography, extraction, mixing, and chemical reactions.[13]

In our previous paper,[14] the phase diagrams, viscosities of the two phases (upper and lower phases) in a batch vessel, volume ratios of the phases, and bright-field or fluorescence photographs of the TRDP were examined by using two-phase separation mixed solvent solutions. However, comprehensive information about the factors influencing the configuration of the inner and outer phases in the TRDP is still lacking for various types of mixed solutions. In this paper, the inner and outer phase configuration in TRDP was, for the first time, considered based on the viscous dissipation principle in a fluidic flow using various types of mixed solvent solutions.

Experimental

Reagents and materials

Acetonitrile, ethyl acetate, chloroform, and tetradecafluorohexane were purchased from Wako Pure Chemical Industries, Ltd. (Osaka, Japan). Triton X-100, hexane, potassium hydroxide (KOH), potassium chloride (KCl), and dipotassium hydrogenphosphate (K_2HPO_4) were purchased from Nacalai Tesque, Inc. (Kyoto, Japan). 1-Butyl-3-methylimidazolium chloride ([C_4mim]Cl) and 1-ethyl-3-methylimidazolium methylphosphonate ([C_2mim]MP) were purchased from Tokyo Chemical Industry Co., Ltd. (Tokyo, Japan). Fused silica capillary tubes (inner diameter: 50 or 75 μm) were purchased from GL Science (Tokyo, Japan).

Viscosity measurement

The homogeneous solutions of all the mixed solvent systems were converted in batch vessels into heterogeneous solution systems that comprised two phases—upper and lower—by changing the temperature. The viscosities of the upper and lower solutions were measured with a viscometer (HAAKE RheoScope 1; Thermo Scientific, Sydney, Australia).

Bright-field or fluorescence microscope–charged-couple device (CCD) camera system

The bright-field or fluorescence microscope–CCD camera system was equipped with a fused silica capillary tube (inner diameter: 50 or 75 μm). The fluorescent dye-containing mixed solvent solution that was introduced into the capillary tube was observed using a microscope (BX51; Olympus, Tokyo, Japan) and a CCD camera (JK-TU53H; Toshiba, Tokyo, Japan) for bright-field and fluorescence imaging. For the latter imaging, the microscope was equipped with an Hg lamp and a filter (U-MWU2; excitation wavelength: 330 – 385 nm, emission wavelength: >420 nm). The temperature of the capillary tube was controlled using a thermo-heater (Thermo Plate MATS-555RO; Tokai Hit Co., Shizuoka, Japan).

Results and Discussion

Inner and outer phase configuration in TRDP using various types of two-phase separation mixed solvent solutions

In our previous paper,[14] the phase diagrams, viscosities of the two phases (upper and lower) in a batch vessel, volume ratios of the phases, and bright-field or fluorescence photographs of the TRDP were examined using different two-phase separation mixed solvent solutions such as ternary water–hydrophilic/hydrophobic organic solvent mixed solution (water–acetonitrile–ethyl acetate), water–micelle mixed solution (water–Triton X-100–KCl), water–ionic liquid mixed solution (water-[C_4mim]Cl–KOH, water–[C_4mim]Cl–K_2HPO_4, and water-[C_2mim]MP–K_2HPO_4), and fluorocarbon/hydrocarbon organic solvent mixed solution (tetradecafluorohexane–hexane). The data are partly resummerized as Supporting Information (Figs. S1 – S4). In the present study, in addition to the above two-phase separation mixed solvent solutions, a ternary water–acetonitrile–chloroform mixed solution was examined. The phase diagrams, viscosities of the two phases (upper and lower) in a batch vessel, volume ratios of the phases, and fluorescence photographs of the TRDP for the water–acetonitrile–chloroform system are shown in Fig. 1.

The differences in the viscosity of the upper and lower solutions of the water–acetonitrile–ethyl acetate, water–acetonitrile–chloroform, water–Triton X-100–KCl, water–[C_4mim]Cl–KOH, water-[C_4mim]Cl–K_2HPO_4, and water–[C_2mim]MP–K_2HPO_4 systems were estimated to be approximately 0.42, 0.49, 440, 1.7, 0.22, and 0.73 mPa·s,[14] respectively. The systems could be tentatively classified according to the degree of difference in the viscosity of the upper and lower phases: that is, as large (approximately >0.73 mPa·s) and small (approximately <0.49 mPa·s). A large viscosity difference between the upper and lower phases was observed for the water–Triton X-100–KCl, water-[C_4mim]Cl–KOH, and water-[C_2mim]MP–K_2HPO_4 systems, whereas a small viscosity difference was observed for the water–acetonitrile–ethyl acetate, water–acetonitrile–chloroform, and water–[C_4min]Cl–K_2HPO_4 systems. The data of tetradecafluorohexane–hexane mixed solvent solution was excluded in this study because the solution generated TRDP with the tetradecafluorohexane-rich solution but did not with the hexane-rich solution.

The following finding has become a gateway to the present work in TRDP research. When the difference in viscosity between the two phases was large (approximately >0.73 mPa·s), the phase with the higher viscosity formed as the inner phase regardless of the volume ratio, whereas when the difference was small (approximately <0.49 mPa·s), the phase with the larger volume formed as the inner phase. Figure 2 shows the relationship between the difference in the viscosity between the two phases and the TRDP configuration.

Principle of viscous dissipation[17-20]

In fluid mechanics, viscous dissipation is manifested by the transformation of kinetic energy into thermal energy through fluidic viscosity. The viscous dissipation (E) per unit length in a two-phase flow of solvents a and b is expressed as follows.

$$E = \sum_{j=a,b} \int_{\Omega_j} \left\{ \frac{1}{2} \mu_j (\nabla u_j)^2 \right\} dV \quad (1)$$

Parameter Ω_j refers to the volume occupied by the solvents, and μ_j and u_j represent the viscosity and velocity of the solvents (j = a (for solvent a) or b (for solvent b)), respectively. According to the principle of viscous dissipation, the fluidic flow flows to maintain the solvent distribution that is determined by the minimum value extracted from the equation.

The principle of viscous dissipation is explained for an annular flow formed by immiscible mixed solvents in Fig. 3. The two types of solvents are immiscible and have different viscosities. As depicted in Fig. 3, the annular flow features an inner phase

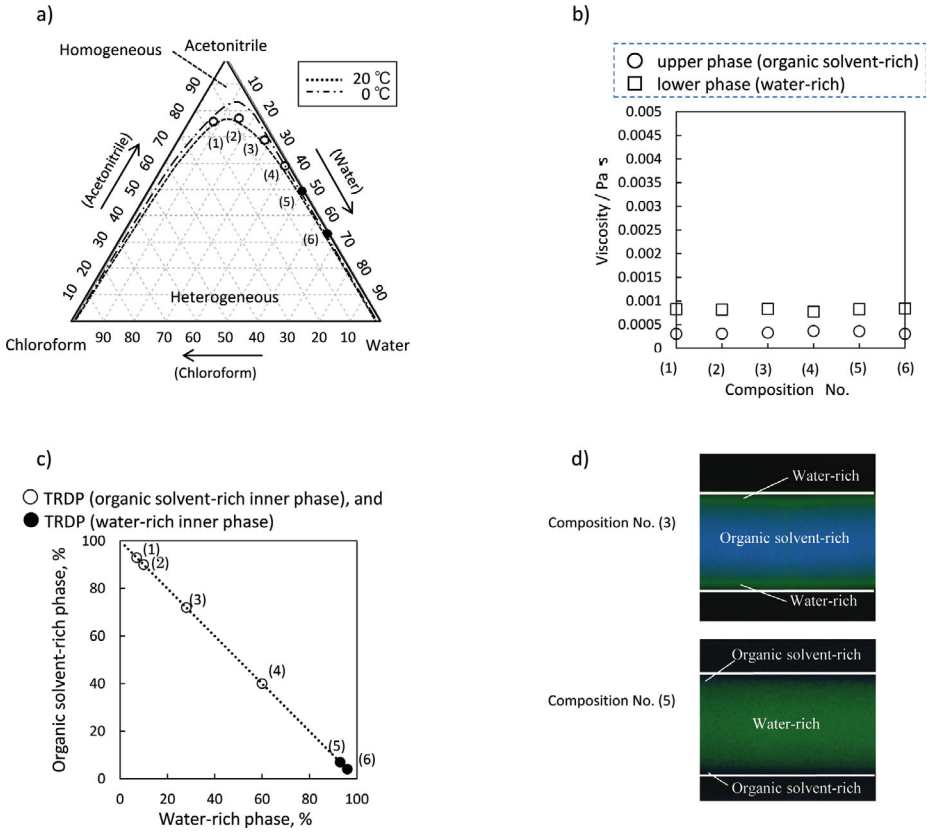

Fig. 1 Results pertaining to the water–acetonitrile–chloroform mixed solvent solution. a) Phase diagrams featuring solubility curves. b) Viscosities of the (○) upper and (□) lower phases in a batch vessel with different solvent compositions denoted by the numbers in brackets in a). c) Relationship between the development of the TRDP and volume contents of the lower and upper phases. Symbols ○ and ● denote the observation of the TRDP (○, organic solvent-rich inner phase and ●, water-rich inner phase). Flow rate, 0.2 µL min^{-1}; temperature, 0°C; capillary tube inner diameter, 50 µm. d) Fluorescence photographs showing the development of the TRDP. Fluorescence dye: 1 mM eosin Y and 0.1 mM perylene. The other conditions are the same as those stated for c).

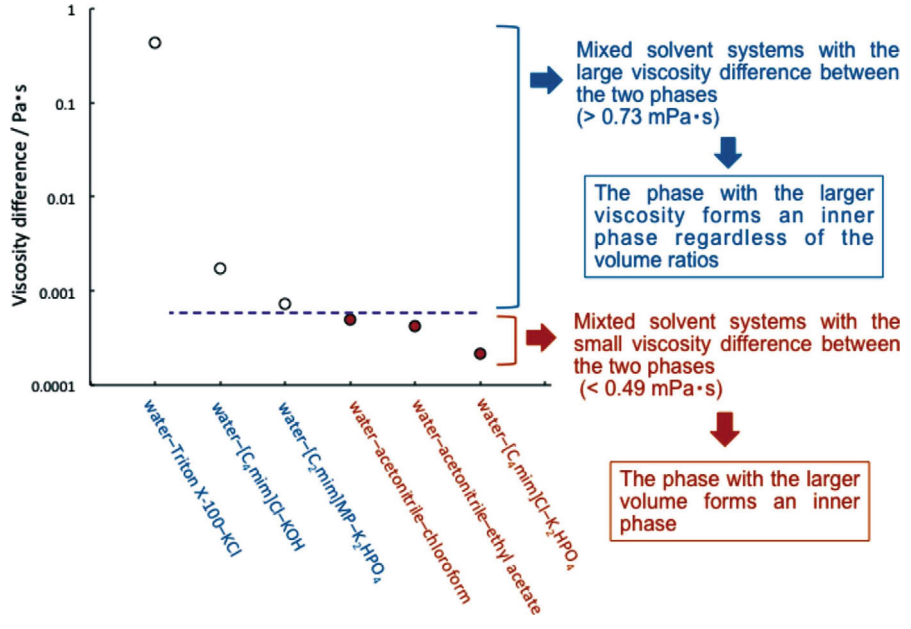

Fig. 2 Viscosity difference between the upper and lower phases for various types of two-phase separation mixed solvent solutions from the viewpoint of inner and outer phases in TRDP. Symbol ○: The phase with the higher viscosity formed as the inner phase regardless of the volume ratio in TRDP. Symbol ●: The phase with the larger volume formed as the inner phase.

and an outer phase, and there are two distribution patterns X and Y. The viscous dissipation energies are estimated with Eq. (1) for the patterns X and Y. For example, an annular flow may form as pattern X when the viscous dissipation energy for pattern X is smaller than that of pattern Y, according to the principle of viscous dissipation.

Equations of viscous dissipation (Eqs. (2) - (25))[20]

To derive concrete equations of viscous dissipation, typical annular flows in an immiscible multi-phase flow, as shown in Fig. 4, were examined. Solvent 1 (with μ_1 and u_o or u_i) and solvent 2 (μ_2 and u_i or u_o) with $\mu_1 < \mu_2$ were introduced as the outer and inner phases, or *vice versa*. Figure 4(a) shows the solvent distribution featuring the higher viscosity solvent as the inner phase and Fig. 4(b) shows the solvent distribution featuring the lower viscosity solvent as the inner phase. The viscous dissipation for the inner (E_i) and outer phases (E_o) is described as follows.

$$E_i = \int_{\Omega_i} \left\{ \frac{1}{2} \mu_i (\nabla u_i)^2 \right\} dV_i = \int_0^{r_{int}} \left\{ \frac{1}{2} \mu_i (\nabla u_i)^2 \right\} \times 2\pi r dr \quad (2)$$

$$E_o = \int_{\Omega_o} \left\{ \frac{1}{2} \mu_o (\nabla u_o)^2 \right\} dV_o = \int_{r_{int}}^{r_{wall}} \left\{ \frac{1}{2} \mu_o (\nabla u_o)^2 \right\} \times 2\pi r dr \quad (3)$$

Parameter r is the radius of the flow in the tube (precisely, r_{int} and r_{wall} are the distances from the center of the tube to the liquid–liquid interface and to the inner wall, respectively, as shown in Fig. 4) and superscripts i and o refer to the inner and outer phases, respectively. The total energy (E_t) can be calculated by combining Eqs. (2) and (3) such that $E_t = E_i + E_o$.

In the case presented in Fig. 4(a), that is, the inner phase is formed by solvent 2 (μ_2 and u_i), and the outer phase is formed by solvent 1 (μ_1 and u_o), first, the velocities of the inner phase (u_i) and outer phase (u_o) are calculated. The viscosities of the inner phase and outer phase are denoted as μ_2 and μ_1, respectively. The equation for describing the velocity of the inner or outer phase is derived from the Navier–Stokes equation of cylindrical coordinate systems (Figs. S5 and S6, Supporting Information) as follows.

$$u = -\frac{\Delta P}{4\mu L} r^2 + C \quad (4)$$

Parameter ΔP is the pressure loss in the capillary, L is the effective length of the capillary, and C is the constant of integration.

Considering the boundary conditions as follows: at the wall surface, $r = r_{wall}$, $u_o = 0$ and at the liquid–liquid interface, $r = r_{int}$, $u_i = u_o$, and G value for convenience, $G = \Delta P/L$, the following equations are obtained.

$$u_i = \frac{G}{4\mu_2}(r_{int}^2 - r^2) + \frac{G}{4\mu_1}(r_{wall}^2 - r_{int}^2) \quad (5)$$

$$u_o = \frac{G}{4\mu_1}(r_{wall}^2 - r^2) \quad (6)$$

When the velocity values are used in the viscous dissipation equation, the following equations are obtained.

$$E_i = \frac{\pi G^2}{16\mu_2} r_{int}^4 \quad (7)$$

$$E_o = \frac{\pi G^2}{16\mu_1}(r_{wall}^4 - r_{int}^4) \quad (8)$$

The total viscous equation energy can then be described as follows.

$$E_t = E_i + E_o = \frac{\pi G^2}{16}\left(\frac{r_{wall}^4 - r_{int}^4}{\mu_1} + \frac{r_{int}^4}{\mu_2} \right) \quad (9)$$

The flow rate, Q, is expressed as follows.

$$Q_j = \int_{\Omega_j} u_j dV_j \quad (10)$$

The flow rates of the inner phase (Q_i) and outer phase (Q_o) are expressed as follows.

$$Q_i = \frac{\pi G}{8\mu_2} r_{int}^4 + \frac{\pi G}{4\mu_1}(r_{wall}^2 r_{int}^2 - r_{int}^4) \quad (11)$$

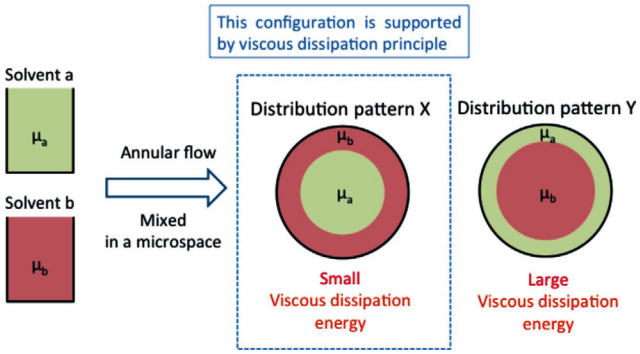

Fig. 3 Schematic illustrating the principle of viscous dissipation for annular flows with immiscible mixed solvents.

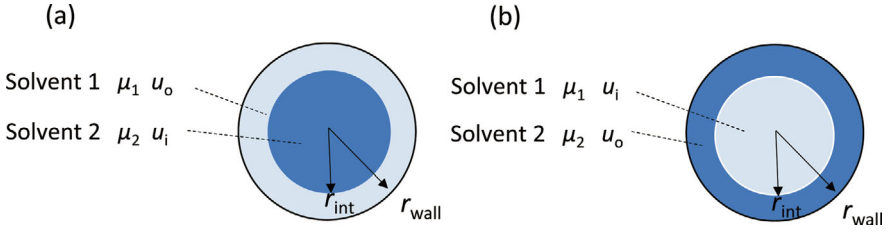

Fig. 4 Typical annular flows generated with solvent 1 (with μ_1 and u_o or u_i) and solvent 2 (μ_2 and u_i or u_o), where ($\mu_1 < \mu_2$), respectively forming as the (a) outer and inner phases or (b) inner and outer phases.

$$Q_o = \frac{\pi G}{8\mu_1}(r_{wall}^4 - 2r_{wall}^2 r_{int}^2 + r_{int}^4) \quad (12)$$

The total flow rate, Q_t, whereby $Q_t = Q_i + Q_o$ can be expressed as follows.

$$Q_t = \frac{\pi G}{8\mu_2} r_{int}^4 + \frac{\pi G}{4\mu_1}(r_{wall}^2 r_{int}^2 - r_{int}^4) + \frac{\pi G}{8\mu_1}(r_{wall}^4 - 2r_{wall}^2 r_{int}^2 + r_{int}^4) \quad (13)$$

Accordingly, G is expressed as follows.

$$G = \frac{8Q_t}{\pi\left(\frac{r_{int}^4}{\mu_2} + \frac{r_{wall}^4 - r_{int}^4}{\mu_1}\right)} \quad (14)$$

Finally, E_t for the case of Fig. 4(a) is expressed as follows.

$$E_t = E_i + E_o = \frac{4{Q_t}^2}{\pi\left(\frac{r_{wall}^4 - r_{int}^4}{\mu_1} + \frac{r_{int}^4}{\mu_2}\right)} \quad (15)$$

In the case presented in Fig. 4(b), that is, the inner phase is formed by solvent 1 (μ_1 and u_i), and the outer phase is formed by solvent 2 (μ_2 and u_o), first, the velocities of the inner (u_i) and outer (u_o) phases are calculated in a similar manner to that for the case shown in Fig. 4(a) as follows.

$$u_1 = \frac{G}{4\mu_1}(r_{int}^2 - r^2) + \frac{G}{4\mu_2}(r_{wall}^2 - r_{int}^2) \quad (16)$$

$$u_o = \frac{G}{4\mu_2}(r_{wall}^2 - r^2) \quad (17)$$

In the above equations, the viscosities of the inner and outer phases are represented as μ_1 and μ_2, respectively. When the velocity values are substituted in the viscous dissipation equation, the following equations are obtained.

$$E_i = \frac{\pi G^2}{16\mu_1} r_{int}^4 \quad (18)$$

$$E_o = \frac{\pi G^2}{16\mu_2}(r_{wall}^4 - r_{int}^4) \quad (19)$$

Accordingly, E_t is expressed as follows.

$$E_t = E_i + E_o = \frac{\pi G^2}{16}\left(\frac{r_{int}^4}{\mu_1} + \frac{r_{wall}^4 - r_{int}^4}{\mu_2}\right) \quad (20)$$

The flow rates of the inner and outer phases are expressed as follows.

$$Q_i = \frac{\pi G}{8\mu_1} r_{int}^4 + \frac{\pi G}{4\mu_2}(r_{wall}^2 r_{int}^2 - r_{int}^4) \quad (21)$$

$$Q_o = \frac{\pi G}{8\mu_2}(r_{wall}^4 - 2r_{wall}^2 r_{int}^2 + r_{int}^4) \quad (22)$$

The total flow rate, Q_t, can be calculated as follows.

$$Q_t = \frac{\pi G}{8\mu_1} r_{int}^4 + \frac{\pi G}{4\mu_2}(r_{wall}^2 r_{int}^2 - r_{int}^4) + \frac{\pi G}{8\mu_2}(r_{wall}^4 - 2r_{wall}^2 r_{int}^2 + r_{int}^4) \quad (23)$$

Parameter G is expressed as follows.

$$G = \frac{8Q_t}{\pi\left(\frac{r_{int}^4}{\mu_1} + \frac{r_{wall}^4 - r_{int}^4}{\mu_2}\right)} \quad (24)$$

Finally, E_t for the case of Fig. 4(b) is expressed as follows.

$$E_t = E_i + E_o = \frac{4{Q_t}^2}{\pi\left(\frac{r_{int}^4}{\mu_1} + \frac{r_{wall}^4 - r_{int}^4}{\mu_2}\right)} \quad (25)$$

Calculation of viscous dissipation

As mentioned above, we examined the TRDP in various types of two-phase separation mixed solvent solutions (Fig. 1, and Figs. S3 and S4 (Supporting Information)) using microscope–CCD camera systems. The viscous dissipation energy for the solution compositions that generated TRDP was calculated for the six types of mixed solvent solutions studied. Specifically, the viscous dissipation energy values for the two distribution patterns shown in Figs. 4(a) and 4(b) were calculated using Eqs. (15) and (25), respectively.

Tables 1 and 2 summarize the values of the viscous dissipation energy obtained for the two distribution patterns together with the component ratios of the solvents and the viscosities of the two phases; the values for the distribution pattern that was actually observed as TRDP are written in red. When the difference in the viscosity between the two phases was large (approximately >0.73 mPa·s) (Table 1), a large difference in the viscous dissipation energy between the solvent distribution patterns was observed. Furthermore, the distribution pattern that was theoretically determined by the viscous dissipation principle corresponded to that actually observed in the photograph in the experiment. Thus, the phase with the higher viscosity formed as the inner phase.

In contrast, when the viscosity difference between the phases was small (approximately <0.49 mPa·s), a small difference in the viscous dissipation energy between the solvent distribution patterns was observed. Furthermore, the distribution pattern of the solvents did not always correspond to the viscous dissipation principle. In other words, the phase with the larger volume formed as the inner phase.

Joseph *et al.*[21] reported the instability of the flow formed by two immiscible liquids with different viscosities in a tube. The experiments showed a tendency for the thinner fluid to encapsulate the thicker fluid. The authors described the distribution pattern by the viscous dissipation principle, which postulated that the extent of viscous dissipation was minimized at a given flow rate. Considering a circular tube, the principle predicted a concentric configuration with the more viscous fluid located at the core. However, a linear stability analysis, as performed by the authors, revealed that though this configuration was stable when the more viscous fluid occupied most of the tube, it was not stable when the tube mostly contained a thinner fluid. Therefore, the authors concluded that the viscous dissipation principle did not always hold, and that the volume ratio of the two fluids was a crucial factor for the configuration in the small viscosity difference between the thicker and thinner ones. The consideration and conclusion of an annular flow formed by an immiscible multi-phase flow by Joseph *et al.* were in accordance with our experimental data and viscous dissipation calculation data of TRDP or TRDF in PS-MPF.

The consideration and conclusion mentioned above could also apply to the experimental data and viscous dissipation calculation data for TRDP that had been reported under the other conditions of inner diameters and flow rates.[13]

Table 1 Viscous dissipation energy data of annular flows for the two distribution patterns shown in Figs. 4(a) and 4(b) when the difference in viscosity between the two phases was large (approximately >0.73 mPa·s) and associated water-rich phase volume ratios

Water rich-phase volume ratio, %	Viscous dissipation energy/$\times 10^{-7}$ J m^{-1} s^{-1}	
	Distribution pattern (a)	Distribution pattern (b)
(a) Water–Triton X-100–KCL[a]		
40	63.4	15700
50	49.4	11400
62	45.4	8770
88	41.2	2160
(b) Water–[C_4mim]Cl–KOH[b]		
20	6.02	8.19
30	5.62	8.03
50	5.18	7.64
70	4.72	7.10
(c) Water–[C_2min]mp–K_2HPO_4[c]		
10	6.75	7.49
35	6.29	7.26
50	6.13	7.28
65	6.12	7.12
90	6.11	6.84

Under these conditions of (a) – (c), the phase with the higher viscosity formed as the inner phase regardless of the volume ratio. The values of the viscous dissipation energy shown in red indicate that TRDP was actually observed in the two distribution patterns.
a. The viscosities of water-rich phase (μ_1), 100 [mPa·s], and surfactant-rich phase (μ_2), 442 [mPa·s].
b. The viscosities of water-rich phase (μ_1), 2.78 [mPa·s], and ionic liquid-rich phase (μ_2), 4.52 [mPa·s].
c. The viscosities of water-rich phase (μ_1), 3.42 [mPa·s], and ionic liquid-rich phase (μ_2), 4.14 [mPa·s].

Table 2 Viscous dissipation energy data of annular flows for the two distribution patterns shown in Figs. 4(a) and 4(b) when the difference in viscosity between the two phases was small (approximately <0.49 mPa·s) and associated water-rich phase volume ratios

Water rich-phase volume ratio, %	Viscous dissipation energy/$\times 10^{-7}$ J m^{-1} s^{-1}	
	Distribution pattern (a)	Distribution pattern (b)
(a) Water–acetonitrile–ethyl acetaste[a]		
10	0.138	0.209
27	0.167	0.262
76	0.198	0.298
90	0.213	0.311
(b) Water–acetonitrile–chloroform[b]		
7	0.111	0.176
28	0.121	0.241
60	0.144	0.264
93	0.197	0.298
96	0.203	0.303
(c) Water–[C_4min]Cl–K_2HPO_4[c]		
5	5.20	5.30
12	5.21	5.40
15	5.30	5.52
35	5.30	5.68
60	5.56	5.98
80	5.75	6.11

Under these conditions of (a) – (c), the phase with the larger volume formed as the inner phase. The values of the viscous dissipation energy shown in red indicate that TRDP was actually observed in the two distribution patterns.
a. The viscosities of organic solvent-rich phase (μ_1), 0.431 [mPa·s], and water-rich phase (μ_2), 0.848 [mPa·s].
b. The viscosities of organic solvent-rich phase (μ_1), 0.335 [mPa·s], and water-rich phase (μ_2), 0.825 [mPa·s].
c. The viscosities of ionic liquid-rich phase (μ_1), 3.00 [mPa·s], and water-rich phase (μ_2), 3.22 [mPa·s].

Conclusions

The current findings are expected to be useful in analytical science including microflow analysis research. The annular flow in PS-MPE, that is, TRDF, was observed using a microscope-CCD camera system; six types of two-phase separation mixed solvent solutions were examined. The viscous dissipation energy was also calculated for the solution component ratios that generated the TRDP. When the difference in viscosity between the two phases was large, the phase with the higher viscosity formed as the inner phase in the TRDP regardless of the volume ratio. The distribution pattern of the solvents was supported by the viscous dissipation principle. In contrast, when the viscosity difference was small, the phase with the larger volume formed as the inner phase in the TRDP. The distribution pattern of the solvents did not always correspond to the viscous dissipation principle. It is interesting and useful to note that the distribution pattern of TRDP or TRDF in PS-MPF could be considered on the basis of the viscous dissipation principle and the report of the linear stability analysis, similarly to that of annular flows in conventional immiscible multi-phase flows.

Acknowledgements

This work was supported by a Grant-in-Aid for Scientific Research (C) from the Ministry of Education, Culture, Sports, Science, and Technology, Japan (MEXT) (No. 26410165).

Supporting Information

The phase diagrams, viscosities of the two phases (upper and lower phases) in a batch vessel, volume ratios of the phases, and bright-field or fluorescence photographs of the TRDP are shown in Figs. S1 – S4, respectively. The schematic diagram of TRDF and the derivation of the velocities equation are shown in Figs. S5 and S6, respectively. These materials are available free of charge on the Web at http://www.jsac.or.jp/analsci/.

References

1. F. F. Reuss, Proceedings of the Imperial Society of Naturalists of Moscow, **1809**, *2*, 327.
2. G. Hagen, *Ann. Phys. Chem.*, **1839**, *46*, 423.
3. R. B. Bird, W. E. Stewart, and E. N. Lightfoot, "*Transport Phenomena*", 2nd ed., **2002**, Chap. 2, Wiley, Toronto.
4. J. W. Jorgenson and K. D. Lukacs, *Anal. Chem.*, **1981**, *53*, 1298.
5. H. Small, *J. Colloid Interface Sci.*, **1974**, *48*, 147.
6. T. Ami, K. Awata, H. Umekawa, and M. Ozawa, *Jpn. J. Multiphase Flow*, **2012**, *26*, 302.
7. H. Foroughi and M. Kawaji, *Int. J. Multiphase Flow*, **2011**, *37*, 1147.
8. M. Kashid and L. K-Minsker, *Chem. Eng. Prog.*, **2011**, *50*, 972.

9. J. Jovanovic, E. V. Rebrov, T. A. X. Nijhuis, M. T. Kretzer, V. Hessel, and J. C. Schouten, *Ind. Eng. Chem. Res.*, **2012**, *51*, 1015.
10. N. Jinno, M. Murakami, K. Mizohata, M. Hashimoto, and K. Tsukagoshi, *Analyst*, **2011**, *135*, 927.
11. M. Murakami, N. Jinno, M. Hashimoto, and K. Tsukagoshi, *Anal. Sci.*, **2011**, *27*, 793.
12. S. Fujinaga, K. Unesaki, S. Negi, M. Hashimoto, and K. Tsukagoshi, *Anal. Methods*, **2012**, *4*, 3884.
13. K. Tsukagoshi, *Anal. Sci.*, **2014**, *30*, 65.
14. S. Fujinaga, K. Unesaki, Y. Kawai, K. Kitaguchi, K. Nagatani, M. Hashimoto, K. Tsukagoshi, and J. Mizushima, *Anal. Sci.*, **2014**, *30*, 1005.
15. S. Fujinaga, M. Hashimoto, K. Tsukagoshi, and J. Mizushima, *J. Chem. Eng. Jpn.*, **2015**, *48*, 947.
16. Y. Hamaguchi, S. Fujinaga, S. Murakami, M. Hashimoto, and K. Tsukagoshi, *Chem. Lett.*, **2014**, *43*, 1318.
17. A. E. Everagae, *Trans. Soc. Rheol.*, **1973**, *17*, 629.
18. J. H. Southern and R. L. Ballman, *Appl. Polymer Symp.*, **1973**, *20*, 175.
19. D. L. Maclean, *Trans. Aoc. Rheol.*, **1973**, *17*, 385.
20. M. C. Williams, *AlChE J.*, **1975**, *21*, 1204.
21. D. D. Joseph, Y. Renardy, and M. Renardy, *J. Fluid Mech.*, **1984**, *141*, 309.